Hindawi
International Journal of Energy Research
Volume 2023, Article ID 5695694, 10 pages
https://doi.org/10.1155/2023/5695694

Research Article

Ultralong-Cycling and Free-Standing Carboxylated Graphene/PEDOT:PSS Films as Electrode for Flexible Supercapacitors

Rongfang Wu,[1,2] Xinjin Xu,[2] Na Li,[2] Congcong Liu,[2,3] Xiao Chen,[2,3] Zhihong Chen,[2] Xiaoqi Lan,[2] Qinglin Jiang,[4] Jingkun Xu,[2] Fengxing Jiang,[2,3] and Peipei Liu[2,3]

[1]*School of Pharmacy, Jiangxi Science and Technology Normal University, Nanchang, 330013 Jiangxi, China*
[2]*Flexible Electronics Innovation Institute, Jiangxi Science and Technology Normal University, Nanchang, 330013 Jiangxi, China*
[3]*Department of Physics, Jiangxi Science and Technology Normal University, Nanchang 330013, China*
[4]*Institute of Polymer Optoelectronic Materials and Devices, State Key Laboratory of Luminescent Materials and Devices, South China University of Technology, Guangzhou 510640, China*

Correspondence should be addressed to Jingkun Xu; xujingkun1971@yeah.net and Peipei Liu; liupeipei8866@126.com

Received 29 September 2022; Revised 17 November 2022; Accepted 23 November 2022; Published 9 February 2023

Academic Editor: Pranav Kalidas Katkar

The rapid development of current wearable electronics motivates the promotion of energy storage devices. Supercapacitor with flexible, lightweight, highly efficient, and long cycling life is one of the potential and glittering candidates. Here, the composite film of carboxylated graphene (CG) and commercially available poly (3, 4-ethylene dioxythiophene): poly (styrene sulfonate) (PEDOT:PSS) are prepared as electrodes for flexible electrochemical capacitors by ultrasonication and vacuum filtration. The CG/PEDOT:PSS films were roundly characterized by SEM, XPS, FTIR, XRD and Raman spectrometer. The as-prepared free-standing films exhibited high specific capacitance (192.7 F g^{-1} at 0.5 A g^{-1}), excellent rate capability (up to 80.4% from 0.5 to 20 A g^{-1}), and good electrochemical stability (95.5% of specific capacitance retention after 50000 cycles). Surprisingly, the post treated free-standing films by Dimethyl Formamide (DMF) shows better capacitive properties than those of the pristine electrode, such as higher specific capacitance (204.3 F g^{-1} at 0.5 A g^{-1}), and ultralong-cycling stability (104.6% retention at a high current density of 20 A g^{-1} after 50000 cycles). It is expected that the free-standing CG/PEDOT:PSS films can be used as flexible electrodes for various wearable energy storage devices.

1. Introduction

Conducting polymers have attracted extensive attention in flexible electronic device applications due to their unique conjugated chain structures, excellent physical, and chemical properties. [1–4] The typical conducting polymers include polyacetylene, polypyrrole, polythiophene, polyaniline, and their derivatives. Among them, as a kind of the derivatives of polythiophene, PEDOT:PSS-based materials have been widely studied, owing to its advantage of conspicuous thermal stability, solution processability, fast charge/discharge kinetics, environmental friendliness, high transparency, and adjustable conductivity ($10^{-4} \sim 10^{3}$ S cm^{-1}). [5–12] However, one of the challenges for the PEDOT:PSS-based materials is their poor cycling stability, which is caused by volume changes during repeated charge-discharge processes (insertion/deintercalation of counter ions). The expansion and contraction of PEDOT:PSS chains may result in structural instability and mechanical degradation, sequentially affecting their capacitive performance. [13, 14] In addition, PEDOT:PSS as an electrode usually suffers from compact morphology, because of its dense growth, limiting its sufficient contact with electrolytes [15, 16].

Graphene, as a popular material in which carbon atoms are connected by sp^2 hybridization, has attracted increasing attention due to its high theoretical surface area and fast electron transportation. [13, 17, 18] But, the near-perfect graphene surface has few active sites. Therefore, a series of methods are applied to change the chemical structure of graphene, such as surface functionalization, chemical doping,

and chemical modification, etc. [19] Carboxylated graphene (CG) is to carboxylate the oxygen-containing groups (epoxy, carbonyl, and hydroxyl) between graphene oxide sheets, increasing the conjugated chain and the active site. The CG with carboxyl groups can easily disperse in water and interact with polymers strongly to form more structurally stable composites. [20] The composites of carboxylated graphene and pseudocapacitive materials possess both physical and mechanical properties. For example, Zhou et al. [21] prepared CG/PPy composite electrodes by the one-pot electrochemical polymerization method. The composite electrode showed a specific capacitance of 170.9 mF cm^{-2} at 0.5 mA cm^{-2}, acceptable cycle stability (96.9% of initial specific capacitance maintained after 5000 cycles), and excellent rate capability. Nonetheless, the reported cycling stability of CG-based composites has not yet met the requirements for supercapacitors in practical application.

In this work, CG/PEDOT:PSS films with high specific capacitance and long-term cycling stability as free-standing electrodes were prepared using a simple sonication and vacuum filtration method. The CG/PEDOT:PSS exhibit better electrochemical properties compared to previously reported electrodes, the main reasons are as follows: (1) PEDOT:PSS enters the CG sheet, which can prevent its stacking, increase the interlayer spacing, and provide a large number of active sites; [22, 23] (2) the interaction between carboxyl groups and PSS chain similar to hydrogen bond, forming cross-linked pores and increasing ion transport channels; and (3) the electrostatic attraction between the $PEDOT^+$ cation and the $-COO^-$ anion makes the composite more stable and spontaneously forms an ordered structure, which is beneficial to the stability during long-term cycling. Besides, the treated electrode by DMF showed a high specific capacitance (204.3 F g^{-1} at 0.5 A g^{-1}), a satisfactory rate capability (80.8% from 0.5 to 20 A g^{-1}), and outstanding cycling stability (the initial specific capacitance retained 104.6% after 50000 cycles).

2. Experimental

2.1. Materials. PEDOT:PSS (Clevios PH1000, PEDOT: PSS = 1 : 2.55, C = 13.6 mg mL^{-1}) was purchased from Heraeus. Carboxylated graphene (CG, C = 2 mg mL^{-1}) was obtained from Nanjing XFNANO Material Tech Co. Ltd. Ethanol (C_2H_5OH, AR, ≥99.7%) and dimethylformamide (DMF, AR, ≥99.5%) were bought from Shanghai Titan Scientific Co., Ltd. Dimethyl sulfoxide (DMSO, AR, ≥99.0%) was acquired from Shanghai Lingfeng Chemical Reagent Co., Ltd. Ethylene Glycol (EG, AR, 99.0%) was achieved from Beijing J&K Scientific Co., Ltd. The water mentioned in the experiment was deionized water (Millipore Co., Ltd.).

2.2. Preparation of CG/PEDOT:PSS. Firstly, a certain amount of PEDOT:PSS was diluted in ethanol with a total volume of 5 mL. Then, mixed the CG and PEDOT:PSS by sonication for 15 mins. For comparison, various ratios of CG and PEDOT:PSS (0 : 2000, 1 : 2000, 2 : 2000, 4 : 2000, 10 : 2000, and 20 : 2000) mixture with a total mass of 5 mg were prepared. The CG/PEDOT:PSS films were obtained by vacuum filtration using PVDF membrane (diameter of 5.0 cm, pore size of 0.45 μm). After stripping in DI water, the films were dried at room temperature and then placed in a 60°C blast oven for 3 h. Finally, a rectangular film of 1 × 1.2 cm was cut with a scalpel for electrochemical testing. The prepared films with different mass ratios of CG and PEDOT:PSS (0 : 2000, 1 : 2000, 2 : 2000, 4 : 2000, 10 : 2000, and 20 : 2000) were denoted as PG_0, PG_1, PG_2, PG_4, PG_{10}, and $PG_{20,}$ respectively.

2.3. Polar Solvent Posttreatment of CG/PEDOT:PSS. To remove excess PSS, PG_1 films were immersed in DMF, DMSO, and EG for 30 mins at room temperature, respectively. The solvent-treated PG_1 films were sequentially rinsed with DI water and C_2H_5OH. After drying in vacuum for 1 h at 80°C, the post-treatment CG/PEDOT:PSS films were acquired. The PG_1 films treated by DMF, DMSO, and EG are denoted as PG_1-M, PG_1-D, and PG_1-E, respectively.

2.4. Materials Characterization. The morphology of the prepared CG/PEDOT:PSS was studied using scanning electron microscopy (SEM, JEOL, JSM-7500F, Japan). Structural characterization was performed by Nicolet Avatar 320 FT-IR spectrometer (Nicolet Instrument Corporation, Madison, WI, USA), UV-visible spectroscopy (SPECORD 200 PLUS), X-ray diffraction (XRD, Rigaku SmartLab SE) and Raman spectroscopy (Horiba Jobin-Yvon Lab-RAM H80). In addition, the elemental and chemical state composition of the CG/PEDOT:PSS films were analyzed by XPS (Thermo Fisher Scientific, USA).

2.5. Electrochemical Measurements. The electrochemical tests in this work were all performed using a CHI660E electrochemical workstation (Shanghai CH Instrument Co., Ltd., China) in 1 M H_2SO_4 electrolyte. Ag/AgCl, CG/PEDOT:PSS films and platinum mesh were used as reference electrodes, working electrodes, and counter electrodes, respectively. The electrochemical properties of CG/PEDOT:PSS films were evaluated by cyclic voltammetry (CV), galvanostatic charge-discharge (GCD), and electrochemical impedance spectroscopy (EIS) measurements.

The specific capacitance (*Cs*) of the film electrode was evaluated according to the GCD curve, which is calculated by the following formula [24]:

$$Cs = \frac{It}{mV} \quad (1)$$

where *I* (A), *t* (s), *m* (g), and *V* (V) are the charge-discharge current, discharge time, the effective mass of the electrode material, and potential window, respectively.

3. Results and Discussion

3.1. Materials Characterization. Figure 1(a) schematically illustrates the preparation process of the CG/PEDOT:PSS composite films. The free-standing films were obtained by two simple steps sonication and vacuum filtration. Then, the composite films were soaked in polar solvent to remove part of the PSS chain. As shown in Figure 1(b), the as-prepared films can be folded, revealing their high flexibility. In addition, it is clear that the pristine PEDOT:PSS film

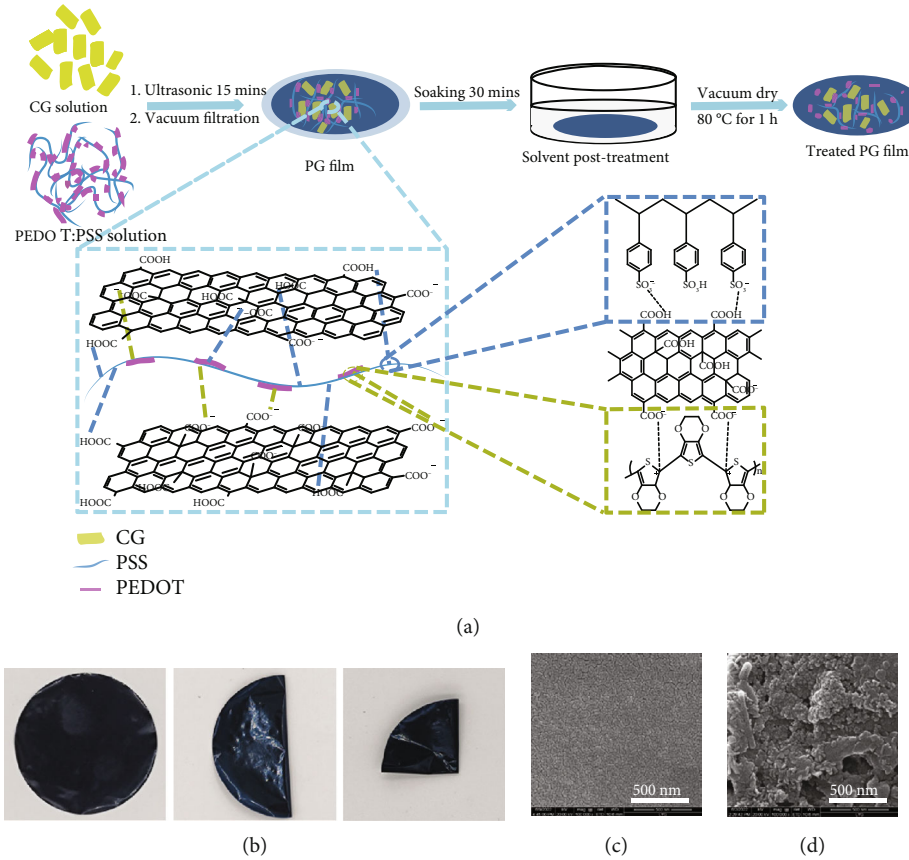

Figure 1: (a) Schematic illustration of the preparation of CG/PEDOT:PSS films. (b) CG/PEDOT:PSS film lay flat, folding once, and folding twice. (c) SEM images of PEDOT:PSS and (d) PG_1 composite film.

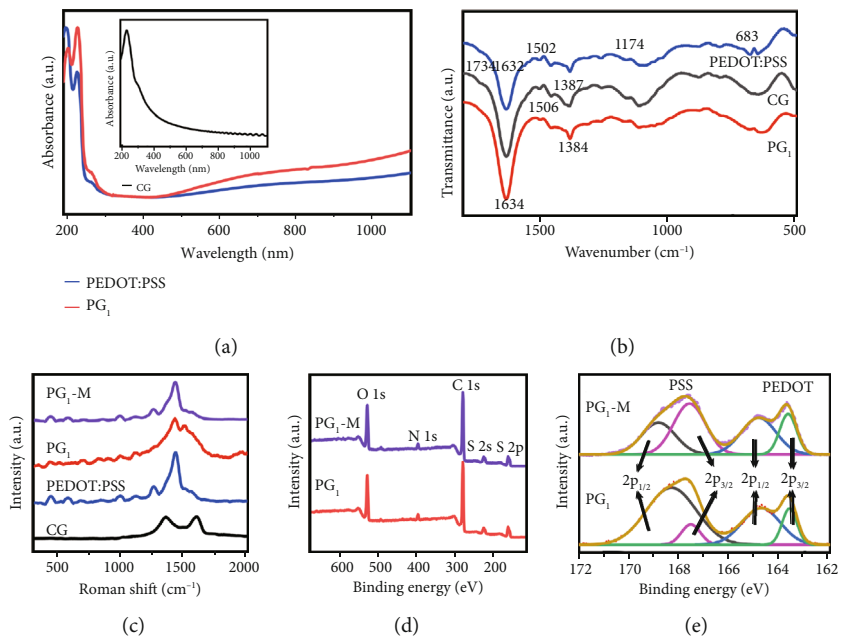

Figure 2: UV-vis absorption spectra (a) and FTIR absorption spectra (b) of CG, PEDOT:PSS, and PG_1 film. (c) Raman spectra of CG, PEDOT:PSS, and PG_1 without and with DMF treatment. (d) The survey XPS spectrum of the PEDOT:PSS and PG_1. (e) XPS spectrum of S 2p of PG_1 before and after DMF treatment.

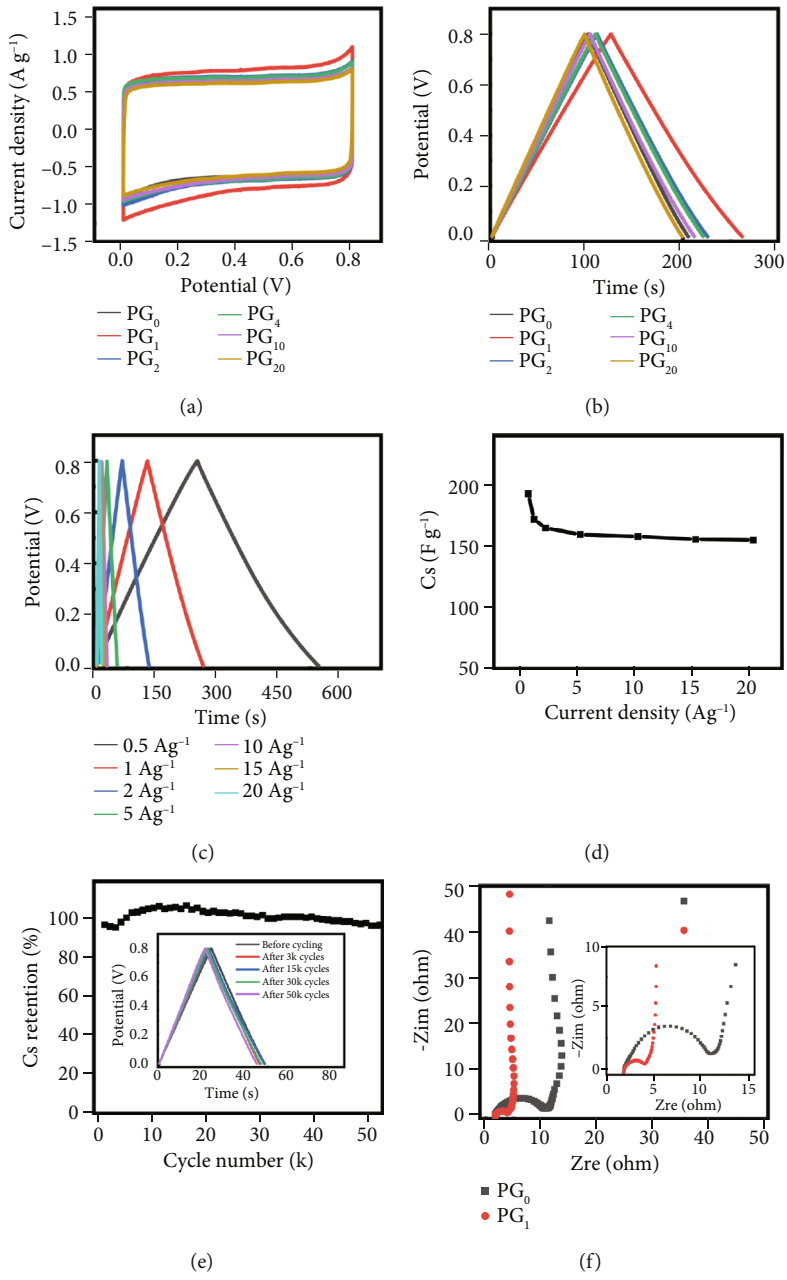

Figure 3: Electrochemical performance of the prepared PG electrodes: (a) CV curves at 5 mV s^{-1}, (b) GCD profiles at 1 A g^{-1}. Capacitive properties of PG1 electrode: (c) GCD profiles at current densities of 0.5, 1, 2, 5, 10, 15, 20 A g^{-1}, (d) Specific capacitance, (e) Cycling stability test (The inset demonstrates the GCD plots before and after 3000, 15000, 30000 and 50000 charge-discharge cycles at 5 A g^{-1}), (f) The Nyquist plots of PG_0 and PG_1 (The inset shows a magnified high-frequency region).

exhibits dense smooth surface, while the PG_1 film possesses numerous spherical particles with uneven size and macropores in the polymer matrix, as exhibited in Figures 1(c) and (d), implying that the addition of CG may affect the chemical properties of the prepared composite film [25].

Figure 2(a) demonstrates the UV-vis spectra of CG, PEDOT:PSS, and PG_1 films. Obviously, CG possesses a characteristic peak at 228 nm and an acromion at 294 nm, which are credited to π-π^* transition of aromatic C – C bonds and $n - \pi^*$ transition of C = O bonds, respectively [26–28]. The two absorption bands of PEDOT:PSS originate from the aromatic rings of PSS at 195 and 225 nm, and the broad peaks at 400~1100 nm are neutral states of PEDOT monopolarons and bipolarons. [28–32] The absorption spectrum of the PG_1 exhibits the characteristic peaks of both the CG and PEDOT:PSS, confirming the successful preparation of the composite film.

Figure 2(b) presents the FT-IR spectra of CG, PEDOT:PSS, and PG_1 film. The characteristic peaks at 1734, 1632, and 1387 cm^{-1} of CG can be seen, which correspond to the carboxyl group C=O, stretching vibrations corresponding to C = C and – COO– bending vibration, respectively, confirming that CG contained carboxylic and carbon-carbon double bond, respectively. [26, 33] For the PEDOT:PSS film, there

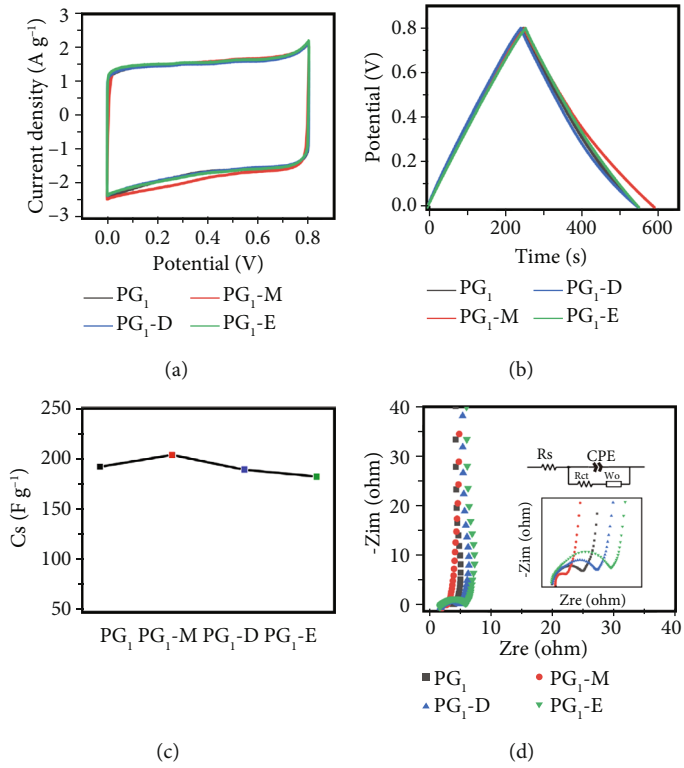

FIGURE 4: Comparisons of electrochemical performance of PG_1, PG_1-M, PG_1-D, and PG_1-E: (a) CV curves at 5 mV s^{-1}, (b) GCD curves at 0.5 A g^{-1}, (c) Specific capacitance at 0.5 A g^{-1}, and (d) Nyquist plot (the inset shows the magnified view of the high-frequency region of the impedance spectra and fitting electrical equivalent circuit).

are two obvious characteristic peaks at 1632 cm^{-1} (C = C alkane stretching vibration peak) and 1502 cm^{-1} (C = C aromatic stretching vibration peak), respectively. Moreover, the peaks at 1174 and 683 cm^{-1} are ascribed to the C – S stretching vibrations on the PSS ring. [34, 35] The vibrational bands can be observed for PG_1, the characteristic peak of –COO– shifted from 1387 to 1384 cm^{-1}, which may result from the π-π stacking of CG and PEDOT:PSS [36].

The structural changes of CG, PEDOT:PSS, and PG_1 composite films were characterized by Raman spectroscopy. The Raman spectrum of the CG in Figure 2(c) demonstrates the presence of D (1350 cm^{-1}) and G band (1591 cm^{-1}). The D band originates from sp^3 vibrations of defective and disordered carbon atoms, and the G band can be attributed to the sp^2 vibration of carbon atoms in a 2D hexagonal lattice. [37–39] In the spectrum of PEDOT:PSS, the main peaks at 437, 676, 575 and 988, 1108, 1256, 1424, 1503, and 1553 cm^{-1} can be ascribed to SO_2 bending, symmetric C – S – C deformation, oxyethylene ring deformation, C – O – C deformation, C – C interring stretching, C = C symmetrical stretching, C=C asymmetrical stretching, and C = C antisymmetrical stretching, respectively. [40, 41] However, the intensity of the peak of PSS is weak, because a part of PSS is carried away by the solvent during the preparation process. In the Raman spectrum of PG_1, the peak related to C = C symmetrical stretching transformed from 1424 to 1421 cm^{-1}, further indicating the successful preparation of the CG/PEDOT:PSS composites. The X-ray diffraction patterns of the PEDOT:PSS, CG, and PG_1 films are presented in Figure S1. The PEDOT:PSS peak in the XRD of PG_1 is shifted and the diffraction peak of CG almost disappears, demonstrating that CG may be wrapped, further suggesting π-π superposition and electrostatic interactions between PEDOT:PSS and CG [42].

The surface chemistry of PG_1 film was further investigated by XPS. There are four elements in the full spectrum, i.e. C, N, O, and S, as shown in Figure 2(d). Element N comes from the carboxyl graphene branch chain. The S element has two different types of peaks: the $S2p_{3/2}$ and $S2p_{1/2}$ peaks at 168.1 eV and 169.4 eV correspond to the element S in PSS sulfonic group, and the doublet $S2p_{3/2}$ and $S2p_{1/2}$ peaks at 163.7 eV and 165.1 eV represent the PEDOT ring of the element S in the thiophene, respectively. [35, 43–45] As displayed in Figure 2(e), the ratios of PEDOT and PSS in PG_1 and PG_1-M films were 0.71 and 0.62, respectively, which were calculated by the peak area of S 2p spectra, confirming partial removal of PSS during solvent treatment process [46, 47].

3.2. Electrochemical Measurements. To investigate the electrochemical properties of PG films, the electrochemical properties of CG were tested, and the composite with different weight ratios of CG and PEDOT:PSS was prepared. As shown in Figure S2, the specific capacitance of pure CG at 1 A g^{-1} is only 10.4 F g^{-1}. The CV curves of PG film with different CG contents (PG_0, PG_1, PG_2, PG_4, PG_{10}, and PG_{20}) at 5 mV s^{-1} are shown in Figure 3(a). All CV curves exhibit regular rectangle characteristics, implying their remarkable capacitive properties. Figure 3(b) displays the GCD plots of

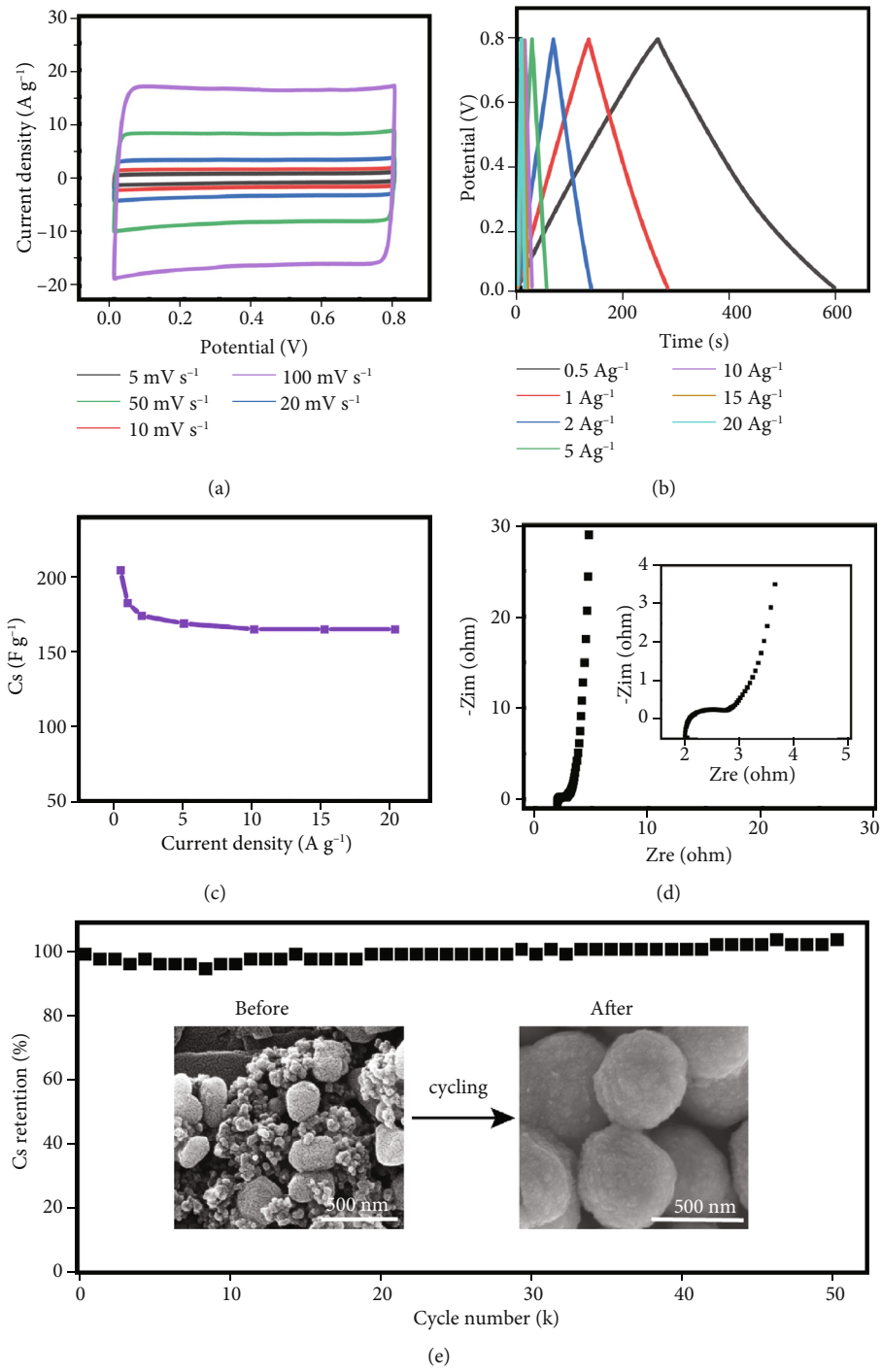

Figure 5: Electrochemical performance of the PG_1-M film in 1 M H_2SO_4 electrolyte: (a) CV curves at 5, 10, 20, 50, and 100 mV s^{-1} scan rates, (b) GCD profiles at current densities of 0.5, 1, 2, 5, 10, 15, and 20 A g^{-1}, (c) specific capacitance at different current densities, (d) Nyquist plot (the inset shows a magnified high-frequency region), and (e) cycling stability study during 50000 charge-discharge cycles (the inset shows SEM images of the PG_1-M electrode before and after cycling.).

the composites at 1 A g^{-1}. Obviously, PG_1 shows a longer discharge time, indicating that the interaction between CG and PEDOT:PSS contributes to the improvement of capacitive performance. The GCD curves of PG_1 are exhibited in Figure 3(c) under potential window of 0 ~ 0.8 V. It is can be seen that the GCD curve still maintains a regular isosceles triangle even at a high current density of 20 A g^{-1}, which further proves the outstanding capacitive performance of PG_1 electrode. Figure 3(d) shows the calculated specific capacitances of PG_1 based on the GCD curves, revealing remarkable rate capability of 80.4% from 0.5 to 20 A g^{-1}. In addition, the PG_1 film shows similar discharge time under 0, 90, and 180° bends, suggesting the good flexibility of the prepared electrode, as displayed in Figure S3.

Table 1: Capacitive performance comparisons of PG_1-M with previously reported conducting polymer based-materials electrode materials.

Electrode materials	*Cs* ($F g^{-1}$)	Current density ($A g^{-1}$)	Retention (cycles)	Ref.
PPy/GO	144	2	91.2% at 0.5 A g^{-1} (4000)	42
PEDOT:PSS	59	10	82.1% at 10 A g^{-1} (5000)	54
PEDOT:PSS:EG/rGO	174	0.5	90% at 0.5 A g^{-1} (5000)	55
PEDOT:PSS/rGO	160	10	91% at 5 A g^{-1} (5000)	56
G-COOZn	238	0.05	>95% at 0.05 A g^{-1} (500)	57
PTh/MWCNT	110	1	90% at 1 A g^{-1} (1000)	58
PEDOT:PSS/rGO	62	1	95% at 1 A g^{-1} (10000)	59
PG_1-M	204.3 165	0.5 20	104.6% at 20 A g^{-1} (50000)	This work

Note: GO: graphene oxide; rGO: reduced graphene oxide; G-COOZn: carboxylated graphene/ZnO; MWCNT: multi-walled carbon nanotubes.

The long-term cycling stability of electrode materials is an essential parameter for electrochemical evaluation. As demonstrated in Figure 3(e), the PG_1 composite electrode exhibits splendid cycling stability after 50000 charge-discharge cycles at 5 A g^{-1} with specific capacitance retention of 95.5%, which is better than those of the PEDOT:PSS, as reported in our previous work. [48] The superior capacitive property can be attributed to the electrostatic attraction of ions and the covalent connections between CG and PEDOT:PSS. The inset of Figure 3(e) shows the GCD curves before and after 3000, 15000, 30000, and 50000 charge-discharge cycles. Apparently, the discharge time under the GCD curve decreases first, then increases, and finally decreases slowly. In the first 3000 cycles, the capacitance decreased, probably because the ion/electron transport channel was not fully open. With the continuous insertion and extraction of ions, the transport channel was opened during the cycling process, facilitating adequate contact between the electrolyte and the electrode material. Meanwhile, the addition of CG gave enough space for the expansion and contraction of PEDOT:PSS. [49, 50] Finally, as the number of cycles increases, the active material is continuously depleted, resulting in a decrease in electrode capacitance. Figure 3(f) exhibits the Nyquist plots of PG_0 and PG_1 in the frequency range from 10^5 to 10^{-2} Hz. The PG_1 electrode shows a solution resistance value (R_s) of 1.7 Ω, which consist of the electronic resistance of the electrode and the ionic resistance of the electrolyte, suggesting that the PG_1 electrode has a high conductivity. [51] The near-vertical line in the low-frequency region manifests remarkable capacitive behavior. Furthermore, the relatively small semicircle of the PG_1 electrode seen in the high-frequency region indicates a lower charge transfer resistance (R_{ct}), as shown in the inset of Figure 3(f). The pure PEDOT:PSS film shows very similar Nyquist plots to PG_1, but it possesses a lower slope in the low-frequency region and a larger semicircle in the high-frequency region, which could account for their poor capacitive performance. In short, the free-standing PG_1 electrode shows better capacitive properties compared to those of other prepared materials. Therefore, PG_1 was selected for further electrochemical investigations.

To achieve better electrochemical performance, the PG_1 films were treated with various polar solvents (DMF, DMSO, EG). The CV curves of the PG_1 films show regular rectangles, indicating that they have good capacitive performance, as displayed in Figure 4(a). Figure 4(b) shows the GCD behaviors of all films at 0.5 A g^{-1}. And the corresponding specific capacitance of PG_1, PG_1-M, PG_1-D, and PG_1-E calculated by the formula (1) are 192.7, 204.3, 189.8, and 183.1 $F g^{-1}$, respectively, as can be seen from Figure 4(c). The results show that PG_1-M has the highest *Cs*, which may be because the treated PEDOT turns into the quinoid structure, which is more favorable for charge transfer [52].

Although the films treated with DMSO and EG have the same effect as above, their *Cs* was not improved. Probably because the films treated by DMSO and EG become more compact, which is not conducive to the transport of charges, resulting in a slight decrease of *Cs*. [48] The EIS curves and fitted equivalent circuit diagrams for the PG_1 electrodes treated by various solvents are shown in Figure 4(d). R_s, CPE, R_{ct}, and W_o represent the solution resistance, double-layer capacitance, charge transfer resistance, and diffusion-controlled Warburg impedance, respectively. As listed in Table S1, the PG_1 treated by DMF in the high-frequency region has the lowest R_{ct}, implying the highest capacitive properties of the PG_1-M electrode compared to those of PG_1, PG_1-D, and PG_1-E.

The electrochemical properties of PG_1-M were further systematically investigated. The CV curves retain their rectangular shape even at a high scan rate of 100 mV s^{-1}, signifying favorable fast charge-discharge kinetics of the PG_1-M electrode, as exhibited in Figure 5(a). The GCD profiles with negligible voltage drop also demonstrate fast charge transfer and ion transport of the electrode (Figure 5(b)). As shown in Figure 5(c), the rate capability of PG_1-M is as high as 80.8% from the current density of 0.5 to 20 A g^{-1}.

The Nyquist plot in Figure 5(d) shows a semicircle with a small radius in the high-frequency region, indicating the low charge transfer impedance of the PG_1-M electrode. The almost perpendicular line in the low-frequency region verifies the fast transport of ions during the charging-discharging of the treated electrode. The cycling stability of the PG_1 composite treated by DMF is evaluated, as displayed in Figure 5(e), manifesting that the initial specific capacitance retention rate reaches 104.6% after 50000 cycles even at a high current density of 20 A g^{-1}. Probably because with the continuous charging and discharging, more and more active sites appear, enhancing the specific capacitance. [48]

Exhilaratingly, the capacitive properties of the treated PG_1-M electrode are better than those of reported conducting polymer based-materials, as listed in Table 1. The possible reasons for the satisfactory capacitive performance of the treated composite are as followings: (1) the DMF solvent can remove parts of the PSS, accommodating large volumetric expansion and contraction during charging-discharging and alleviating degradation of PEDOT:PSS [47, 51] ; (2) the exposed active sites of the treated free-standing films increased with the continuous cycles, improving the specific capacitance of the electrode; and (3) there is still a part of PSS that may be removed during the charging and discharging process, which makes the film surface rougher, increasing the specific capacitance [48, 53].

4. Conclusions

The free-standing CG/PEDOT:PSS films were obtained by simple sonication and vacuum filtration steps. The prepared free-standing electrode shows an acceptable specific capacitance of 192.7 F g^{-1} at 0.5 A g^{-1} and superior cycling stability with 95.5% capacitance retention after 50000 charge-discharge cycles at 5 A g^{-1}. The remarkable electrochemical performance can be ascribed to the interaction between the CG and PEDOT:PSS. More excitingly, the treated CG/PEDOT:PSS electrode by DMF displays a better capacitive performance compared to the pristine film. In particular, the treated film demonstrates superior cycling stability (104.6% retention after 50000 cycles at 20 A g^{-1}) than previously reported conductive polymer-based electrode materials. In sum, this investigation provides the possibility to achieve capacitive electrodes with ultralong cycle life and satisfactory specific capacitance for energy storage devices.

Data Availability

Data available in article.

Conflicts of Interest

There is no conflict of interest between the authors.

Acknowledgments

This work was supported by the National Natural Science Foundation of China (No. 52073128, 51762018, 22065013, 52272214, and 52203221), Natural Science Foundation of Guangdong Province (No. 2022A1515010063), Basic and Applied Basic Research Program of Guangzhou (No. 202102020401), Natural Science Foundation of Jiangxi Province, China (No. 20202ACBL204005, 20202ACBL214005, 20203AEI003, and 20212BAB214017), and Foundation of Jiangxi Science and Technology Normal University (No. 2019BSQD001).

Supplementary Materials

Details of the XRD, flexibility, and CG electrochemical properties of the composite films are given in the supplementary material. *(Supplementary Materials)*

References

[1] B. W. Yao, H. Y. Wang, Q. Q. Zhou et al., "Ultrahigh-conductivity polymer hydrogels with arbitrary structures," *Advanced Materials*, vol. 29, no. 28, p. 1700974, 2017.

[2] H. M. Wang, H. R. Yang, Y. F. Diao, Y. Lu, K. Chrulski, and J. M. D'Arcy, "Solid-state precursor impregnation for enhanced capacitance in hierarchical flexible poly(3,4-ethylenedioxythiophene) supercapacitors," *ACS Nano*, vol. 15, no. 4, pp. 7799–7810, 2021.

[3] Q. Q. Zhou and G. Q. Shi, "Conducting polymer-based catalysts," *Journal of the American Chemical Society*, vol. 138, no. 9, pp. 2868–2876, 2016.

[4] Y. H. Wang, X. Chu, Z. H. Zhu, D. Xiong, H. T. Zhang, and W. Q. Yang, "Dynamically evolving 2D supramolecular polyaniline nanosheets for long- stability flexible supercapacitors," *Chemical Engineering Journal*, vol. 423, article 130203, 2021.

[5] A. I. Hofmann, W. T. T. Smaal, M. Mumtaz et al., "An alternative anionic polyelectrolyte for aqueous PEDOT dispersions: toward printable transparent electrodes," *Angewandte Chemie International Edition*, vol. 54, no. 29, pp. 8506–8510, 2015.

[6] X. T. Hu, L. Chen, Y. Zhang, Q. Hu, J. L. Yang, and Y. W. Chen, "Large-scale flexible and highly conductive carbon transparent electrodes via roll-to-roll process and its high performance lab-scale indium tin oxide-free polymer solar cells," *Chemistry of Materials*, vol. 26, no. 21, pp. 6293–6302, 2014.

[7] Q. S. Wei, M. Mukaida, Y. Naitoh, and T. Ishida, "Morphological change and mobility enhancement in PEDOT:PSS by adding co- solvents," *Advanced Materials*, vol. 25, no. 20, pp. 2831–2836, 2013.

[8] K. V. D. Ruit, R. I. Cohen, D. Bollen et al., "Quasi-one dimensional in-plane conductivity in filamentary films of PEDOT:PSS," *Advanced Functional Materials*, vol. 23, no. 46, pp. 5778–5786, 2013.

[9] N. Kim, B. H. Lee, D. Choi et al., "Role of interchain coupling in the metallic state of conducting polymers," *Physical Review Letters*, vol. 109, no. 10, article 106405, 2012.

[10] Q. Zhao, J. Y. Liu, Z. X. Wu et al., "Robust PEDOT:PSS-based hydrogel for highly efficient interfacial solar water purification," *Chemical Engineering Journal*, vol. 442, article 136284, 2022.

[11] Z. H. Wang, P. Tammel, J. X. Huo, P. Zhang, M. Strømme, and L. Nyholm, "Solution-processed poly(3,4-ethylenedioxythiophene) nanocomposite paper electrodes for high-capacitance flexible supercapacitors," *Journal of Materials Chemistry A*, vol. 4, no. 5, pp. 1714–1722, 2016.

[12] L. Groenendaal, F. Jonas, D. Freitag, H. Pielartzik, and J. R. Reynolds, "Poly(3,4-ethylenedioxythiophene) and its derivatives: past, present, and future," *Advanced Materials*, vol. 12, no. 7, pp. 481–494, 2000.

[13] K. Wang, H. P. Wu, Y. N. Meng, and Z. X. Wei, "Conducting polymer nanowire arrays for high performance supercapacitors," *Small*, vol. 10, no. 1, pp. 14–31, 2014.

[14] H. H. Zhou and X. M. Zhi, "Ternary composite electrodes based on poly(3,4-ethylenedioxythiophene)/carbon nanotubes-carboxyl graphene for improved electrochemical capacitive performances," *Synthetic Metals*, vol. 234, pp. 139–144, 2017.

[15] Y. Zhou, H. P. Xu, N. Lachman et al., "Advanced asymmetric supercapacitor based on conducting polymer and aligned carbon nanotubes with controlled nanomorphology," *Nano Energy*, vol. 9, pp. 176–185, 2014.

[16] Y. Shi, L. L. Peng, Y. Ding, Y. Zhao, and G. H. Yu, "Nanostructured conductive polymers for advanced energy storage," *Chemical Society Reviews*, vol. 44, no. 19, pp. 6684–6696, 2015.

[17] Y. Liu, R. J. Deng, Z. Wang, and H. T. Liu, "Carboxyl-functionalized graphene oxide-polyaniline composite as a promising supercapacitor material," *Journal of Materials Chemistry*, vol. 22, no. 27, pp. 13619–13624, 2012.

[18] M. Athanasiou, S. N. Yannopoulos, and T. Ioannides, "Biomass-derived graphene-like materials as active electrodes for supercapacitor applications: a critical review," *Chemical Engineering Journal*, vol. 446, article 137191, 2022.

[19] L. Dong, J. Yang, M. Chhowalla, and K. P. Loh, "Synthesis and reduction of large sized graphene oxide sheets," *Chemical Society Reviews*, vol. 46, no. 23, pp. 7306–7316, 2017.

[20] T. Szabó, E. Tombácz, E. Illés, and I. Dékány, "Enhanced acidity and pH-dependent surface charge characterization of successively oxidized graphite oxides," *Carbon*, vol. 44, no. 3, pp. 537–545, 2006.

[21] H. Zhou and H. J. Zhai, "Boosting the electrochemical capacitive properties of polypyrrole using carboxylated graphene oxide as a new dopant," *Journal of Materials Science: Materials in Electronics*, vol. 29, no. 9, pp. 7893–7903, 2018.

[22] T. Xu, D. Z. Yang, S. Y. Zhang, T. Y. Zhao, M. Zhang, and Z. Z. Yu, "Antifreezing and stretchable all-gel-state supercapacitor with enhanced capacitances established by graphene/PEDOT-polyvinyl alcohol hydrogel fibers with dual networks," *Carbon*, vol. 171, pp. 201–210, 2021.

[23] W. L. Teng, Q. Q. Zhou, X. K. Wang et al., "Enhancing ions/electrons dual transport in rGO/PEDOT:PSS fiber for high- performance supercapacitor," *Carbon*, vol. 189, pp. 284–292, 2022.

[24] W. F. Liu, S. C. Luo, D. Liu et al., "Facile processing of free-standing polyaniline/SWCNT film as an integrated electrode for flexible supercapacitor application," *ACS Applied Materials & Interfaces*, vol. 9, no. 39, pp. 33791–33801, 2017.

[25] S. Lehtimäki, M. Suominen, P. Damlin, S. Tuukkanen, C. Kvarnström, and D. Lupo, "Preparation of supercapacitors on flexible substrates with electrodeposited PEDOT/graphene composites," *ACS Applied Materials & Interfaces*, vol. 7, no. 40, pp. 22137–22147, 2015.

[26] H. H. Zhou, H. J. Zhai, and X. M. Zhi, "Enhanced electrochemical performances of polypyrrole/carboxyl graphene/carbon nanotubes ternary composite for supercapacitors," *Electrochimica Acta*, vol. 290, pp. 1–11, 2018.

[27] K. Zhang, N. Heo, X. J. Shi, and J. H. Park, "Chemically modified graphene oxide-wrapped quasi-micro ag decorated silver trimolybdate nanowires for photocatalytic applications," *Journal of Physical Chemistry C*, vol. 117, no. 45, pp. 24023–24032, 2013.

[28] R. Imani, S. H. Emami, and S. Faghihi, "Nano-graphene oxide carboxylation for efficient bioconjugation applications: a quantitative optimization approach," *Journal of Nanoparticle Research*, vol. 17, no. 2, p. 88, 2015.

[29] M. Culebras, C. M. Gómez, and A. Cantarero, "Enhanced thermoelectric performance of PEDOT with different counter-ions optimized by chemical reduction," *Journal of Materials Chemistry A*, vol. 2, no. 26, pp. 10109–10115, 2014.

[30] Y. J. Xia, K. Sun, and J. Y. Ouyang, "Highly conductive poly(3,4-ethylenedioxythiophene):poly(styrene sulfonate) films treated with an amphiphilic fluoro compound as the transparent electrode of polymer solar cells," *Energy & Environmental Science*, vol. 5, no. 1, pp. 5325–5332, 2012.

[31] H. Huang, L. C. Xia, Y. P. Zhao et al., "Three-dimensional porous reduced graphene oxide/PEDOT:PSS aerogel: facile preparation and high performance for supercapacitor electrodes," *Electrochimica Acta*, vol. 364, article 137297, 2020.

[32] D. Alemu, H. Y. Wei, K. C. Ho, and C. W. Chu, "Highly conductive PEDOT:PSS electrode by simple film treatment with methanol for ITO-free polymer solar cells," *Energy & Environmental Science*, vol. 5, no. 11, pp. 9662–9671, 2012.

[33] S. V. Sadavar, N. S. Padalkar, R. B. Shinde et al., "Graphene oxide as an efficient hybridization matrix for exploring electrochemical activity of two-dimensional cobalt-chromium-layered double hydroxide-based nanohybrids," *ACS Applied Energy Materials*, vol. 5, no. 2, pp. 2083–2095, 2022.

[34] X. L. Mao, W. Y. Yang, X. He et al., "The preparation and characteristic of poly (3,4-ethylenedioxythiophene)/reduced graphene oxide nanocomposite and its application for supercapacitor electrode," *Materials Science and Engineering B*, vol. 216, pp. 16–22, 2017.

[35] G. Q. Liu, X. Chen, C. C. Liu et al., "DMSO-treated flexible PEDOT:PSS/PANi fiber electrode for high performance supercapacitors," *Journal of Materials Science*, vol. 56, no. 26, pp. 14632–14643, 2021.

[36] L. Wan, B. Wang, S. M. Wang et al., "Well-dispersed PEDOT:PSS/graphene nanocomposites synthesized by in situ polymerization as counter electrodes for dye-sensitized solar cells," *Journal of Materials Science*, vol. 50, no. 5, pp. 2148–2157, 2015.

[37] Q. F. Zheng, Z. Y. Cai, Z. Q. Ma, and S. Q. Gong, "Cellulose nanofibril/reduced graphene oxide/carbon nanotube hybrid aerogels for highly flexible and all-solid-state supercapacitors," *ACS Applied Materials & Interfaces*, vol. 7, no. 5, pp. 3263–3271, 2015.

[38] N. S. Padalkar, S. V. Sadavar, R. B. Shinde et al., "2D-2D nanohybrids of Ni-Cr-layered double hydroxide and graphene oxide nanosheets: electrode for hybrid asymmetric supercapacitors," *Electrochimica Acta*, vol. 424, article 140615, 2022.

[39] Y. Ma, N. Wei, Q. Wang et al., "Ultrathin PEDOT:PSS/rGO aerogel providing tape-like self-healable electrode for sensing space electric field with electrochemical mechanism," *Advanced Electronic Materials*, vol. 5, no. 12, article 1900637, 2019.

[40] D. Yoo, J. Kim, and J. H. Kim, "Direct synthesis of highly conductive poly(3,4-ethylenedioxythiophene):poly(4-styrenesulfonate) (PEDOT:PSS)/graphene composites and their applications in energy harvesting systems," *Nano Research*, vol. 7, no. 5, pp. 717–730, 2014.

[41] S. Cho, M. Kim, and J. Jang, "Screen-printable and flexible RuO_2 nanoparticle-decorated PEDOT:PSS/graphene nanocomposite with enhanced electrical and electrochemical performances for high-capacity supercapacitor," *ACS Applied Materials & Interfaces*, vol. 7, no. 19, pp. 10213–10227, 2015.

[42] W. L. Wu, L. Q. Yang, S. L. Chen et al., "Core-shell nanospherical polypyrrole/graphene oxide composites for high performance supercapacitors," *RSC Advances*, vol. 5, no. 111, pp. 91645–91653, 2015.

[43] X. Crispin, F. L. E. Jakobsson, A. Crispin et al., "The origin of the high conductivity of poly(3,4-ethylenedioxythiophene)-poly(styrenesulfonate) (PEDOT-PSS) plastic electrodes," *Chemistry of Materials*, vol. 18, no. 18, pp. 4354–4360, 2006.

[44] I. K. Moon, B. Ki, and J. Oh, "Three-dimensional porous stretchable supercapacitor with wavy structured PEDOT:PSS/

graphene electrode," *Chemical Engineering Journal*, vol. 392, article 123794, 2020.

[45] E. J. Bae, H. Y. Kang, K. S. Jang, and S. Y. Cho, "Enhancement of thermoelectric properties of PEDOT:PSS and tellurium-PEDOT:PSS hybrid composites by simple chemical treatment," *Scientific Reports*, vol. 6, no. 1, p. 18805, 2016.

[46] J. Y. Kim, J. H. Jung, D. E. Lee, and J. Joo, "Enhancement of electrical conductivity of poly(3,4-ethylenedioxythiophene)/poly(4-styrenesulfonate) by a change of solvents," *Synthetic Metals*, vol. 126, no. 2-3, pp. 311–316, 2002.

[47] J. Y. Ouyang, Q. F. Xu, C. W. Chu, Y. Yang, G. Li, and J. Shinar, "On the mechanism of conductivity enhancement in poly(3,4-ethylenedioxythiophene):poly(styrene sulfonate) film through solvent treatment," *Polymer*, vol. 45, no. 25, pp. 8443–8450, 2004.

[48] G. Q. Liu, F. X. Jiang, J. Liu et al., "Solvent treatment inducing ultralong cycle stability poly(3,4-ethylenedioxythiophene):poly(styrenesulfonic acid) fibers as binding- free electrodes for supercapacitors," *International Journal of Energy Research*, vol. 44, no. 7, pp. 5856–5865, 2020.

[49] M. Boota, C. Chen, M. Bécuwe, L. Miao, and Y. Gogotsi, "Pseudocapacitance and excellent cyclability of 2,5-dimethoxy-1,4-benzoquinone on graphene," *Energy & Environmental Science*, vol. 9, no. 8, pp. 2586–2594, 2016.

[50] M. Boota and Y. Gogotsi, "MXene—conducting polymer asymmetric pseudocapacitors," *Advanced Energy Materials*, vol. 9, no. 7, p. 1802917, 2019.

[51] X. Y. Chang, M. F. El-Kady, A. Huang et al., "3D Graphene network with covalently grafted aniline tetramer for ultralong-life supercapacitors," *Advanced Functional Materials*, vol. 31, no. 32, article 2102397, 2021.

[52] W. Q. Zhou and J. K. Xu, "High-operating-voltage all-solid-state symmetrical supercapacitors based on poly(3,4-ethylenedioxythiophene)/poly(styrenesulfonate) films treated by organic solvents," *Electrochimica Acta*, vol. 222, pp. 1895–1902, 2016.

[53] Z. F. Li, G. Q. Ma, R. Ge et al., "Free-standing conducting polymer films for high-performance energy devices," *Angewandte Chemie*, vol. 128, no. 3, pp. 991–994, 2016.

[54] Y. Y. Wang, G. Q. Liu, Y. F. Liu et al., "Heterostructural conductive polymer with multi-dimensional carbon materials for capacitive energy storage," *Applied Surface Science*, vol. 558, article 149910, 2021.

[55] S. Khasim, A. Pasha, N. Badi, M. Lakshmi, and Y. K. Mishra, "High performance flexible supercapacitors based on secondary doped PEDOT-PSS-graphene nanocomposite films for large area solid state devices," *RSC Advances*, vol. 10, no. 18, pp. 10526–10539, 2020.

[56] G. Q. Liu, X. Chen, J. Liu et al., "Fabrication of PEDOT:PSS/rGO fibers with high flexibility and electrochemical performance for supercapacitors," *Electrochimica Acta*, vol. 365, article 137363, 2021.

[57] K. W. Park and J. H. Jung, "Spectroscopic and electrochemical characteristics of a carboxylated graphene- ZnO composites," *Journal of Power Sources*, vol. 199, pp. 379–385, 2012.

[58] C. P. Fu, H. H. Zhou, R. Liu, Z. Y. Huang, J. H. Chen, and Y. F. Kuang, "Supercapacitor based on electropolymerized polythiophene and multi-walled carbon nanotubes composites," *Materials Chemistry and Physics*, vol. 132, no. 2-3, pp. 596–600, 2012.

[59] Y. Q. Liu, B. Weng, J. M. Razal et al., "High-performance flexible all-solid-state supercapacitor from large free- standing Graphene-PEDOT/PSS films," *Scientific Reports*, vol. 5, no. 1, p. 17045, 2015.